Applied Surface Science 357 (2015) 771–776

Contents lists available at ScienceDirect

Applied Surface Science

journal homepage: www.elsevier.com/locate/apsusc

Restructured graphene sheets embedded carbon film by oxygen plasma etching and its tribological properties

Meiling Guo[a], Dongfeng Diao[b,*], Lei Yang[a], Xue Fan[b]

[a] Key Laboratory of Education Ministry for Modern Design and Rotor-Bearing System, School of Mechanical Engineering, Xi'an Jiaotong University, Xi'an 710049, China
[b] Institute of Nanosurface Science and Engineering (INSE), Shenzhen University, Shenzhen 518060, China

ARTICLE INFO

Article history:
Received 10 June 2015
Received in revised form 7 September 2015
Accepted 12 September 2015
Available online 15 September 2015

Keywords:
Graphene sheets embedded carbon film
Oxygen plasma etching
Restructuring
Surface roughness
Mechanical properties
Tribological properties

ABSTRACT

An oxygen plasma etching technique was introduced for improving the tribological properties of the graphene sheets embedded carbon (GSEC) film in electron cyclotron resonance plasma processing system. The nanostructural changing in the film caused by oxygen plasma etching was examined by transmission electron microscope, Raman spectroscopy and X-ray photoelectron spectroscopy, showing that the 3 nm thick top surface layer was restructured with smaller graphene nanocrystallite size as well as higher sp^3 bond fraction. The surface roughness, mechanical behavior and tribological properties of the original GSEC and oxygen plasma treated GSEC films were compared. The results indicated that after the oxygen plasma treatment, the average roughness decreased from 20.8 ± 1.1 nm to 1.9 ± 0.1 nm, the hardness increased from 2.3 ± 0.1 GPa to 2.9 ± 0.1 GPa, the nanoscratch depth decreased from 64.5 ± 5.4 nm to 9.9 ± 0.9 nm, and the wear life increased from 930 ± 390 cycles to more than 15,000 frictional cycles. The origin of the improved tribological behavior was ascribed to the 3 nm thick graphene nanocrystallite film. This finding can be expected for wide applications in nanoscale surface engineering.

1. Introduction

Carbon based nano devices have bright prospects in the modern semiconductor industry since they show excellent electrical, optical as well as other performances and can be easily integrated with silicon substrate during fabrication [1,2]. In their applications, many of them involve moving parts, making tribological property of carbon materials a key issue to determine the reliability of devices [3,4]. Nanostructured carbon films with nanocrystallites embedded in the amorphous carbon matrix are expected as candidates for novel carbon based nano devices because the nanocrystallites, such as graphene, graphite, fullerene and nanotubes, possess remarkable and tunable characteristics, which can widen the properties of devices [5–7]. However, the growth of sp^2 clusters in amorphous phase may lead to surface roughening [8,9], which can certainly cause high friction and severe wear losses [10], finally limiting the application prospect of nanostructured carbon films in carbon based nano devices. Recently, a graphene sheets embedded carbon (GSEC) film under the low energy electron irradiation in electron cyclotron resonance (ECR) plasma processing system was developed. This carbon film has been proved to have high electrical conductivity and strong magnetism due to the embedded graphene sheets [11,12]. These outstanding properties made this film become a candidate for potential applications in spintronics and nanoelectromechanical system. However, it was also found that the GSEC film had rough surface, low hardness and relatively poor tribological properties [13], making its application in nano devices restricted.

Plasma treatment, especially oxygen plasma treatment with high chemical reactivity to carbon has become an effective way for the modification of carbon based materials to alter their nanostructures and properties [14–20]. Kim et al. [17] studied oxygen plasma etching induced bond structural evolution of a single layer graphene, and an increasing level of disorder indicated a structural change from a graphene lattice to a more amorphous carbon phase. Jiang et al. [18] reported that oxygen plasma preferentially etched the soft graphite-like sp^2 clusters in sp^3 and sp^2 carbon network. Zheng et al. [19] reported that the etching of diamond films in an oxygen plasma led to a decrease of surface roughness due to the joint action of physical and chemical etching. Our previous work [20] has proved the oxygen plasma etching could improve the scratch resistance of carbon films. Therefore, for the GSEC film, the

* Corresponding author.
E-mail address: dfdiao@szu.edu.cn (D. Diao).

http://dx.doi.org/10.1016/j.apsusc.2015.09.116
0169-4332/

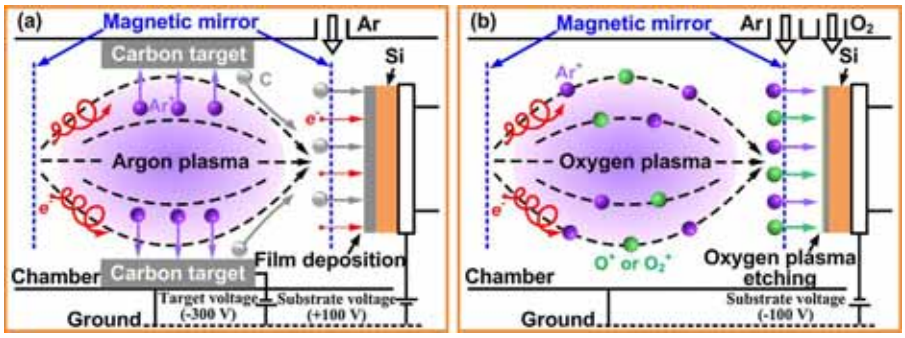

Fig. 1. Schematic diagram of (a) deposition of the GSEC film and (b) oxygen plasma etching (mainly O^+, O_2^+ and Ar^+) process of the GSEC film. (For interpretation of the references to color in the text, the reader is referred to the web version of this article.)

oxygen plasma etching may be an effective modification approach to not only smooth the surface but also improve the mechanical and tribological properties.

In this study, an oxygen plasma etching technique in ECR plasma processing system was proposed as a potential method for improving the tribological properties of the GSEC film. The oxygen plasma treated GSEC film was fabricated by sequential GSEC film deposition and oxygen plasma etching for three times. The nanostructure, surface roughness, mechanical and tribological properties of the GSEC film and the oxygen plasma treated GSEC film were compared for clarifying the effect of oxygen plasma etching and understanding the mechanism of tribological property enhancement.

2. Experiments

2.1. Deposition and oxygen plasma treatment of GSEC film

A mirror confinement ECR plasma processing system was used for the fabrication and the plasma treatment of the GSEC film. Full details of the system have been reported in our previous works [13,21]. Fig. 1 shows the schematic diagram of the film deposition and the oxygen plasma etching procedure. Silicon substrate was cleaned in acetone and ethanol bath successively by ultrasonic wave and then fixed onto the substrate holder. The chamber was evacuated to the pressure of 3×10^{-4} Pa, and working gas was introduced keeping the working pressure to be 0.04 Pa. ECR plasma was generated when the 200 W microwave and the magnetic field were applied, and the electron momentum at the magnetic mirror position (blue dashed lines in Fig. 1) was zero. Then, electron irradiation and ion irradiation were realized by applying a positive and a negative bias voltage on the substrate holder, respectively. Fig. 1(a) presents the GSEC film deposition process, and the working gas was argon. With a target discharge voltage of −300 V, argon ions were attracted to the carbon target to sputter the target surface, providing carbon atoms for the film growth. At the same time, a low energy electron irradiation (100 eV) was realized by applying a substrate bias voltage of +100 V, and the electron irradiation density was 72 mA/cm^2. The deposition rate of carbon film was about 8 nm/min. After that, as shown in Fig. 1(b), oxygen and argon gaseous mixture with oxygen gas concentration of 12% was injected into the chamber to generate the oxygen plasma, and the target voltage was set to zero. With a substrate bias voltage of −100 V, the O^+, O_2^+ and Ar^+ were extracted to etch the as-deposited carbon film, and the etching thickness was 40 nm in 1 min. In this study, the GSEC film was firstly deposited for 15 min and the film thickness was around 120 nm. Then this carbon film was etched by oxygen plasma for 1 min and the film thickness decreased to around 80 nm. By repeating this sequential film deposition and plasma etching process for three times, the oxygen plasma treated GSEC film with thickness of around 240 nm was obtained. The GSEC film with comparable thickness was fabricated through 30 min film deposition for comparison.

2.2. Film characterization

The nanostructures of the carbon films were directly observed by a JEM-2100 transmission electron microscope (TEM) operated with the electron acceleration voltage of 200 kV. TEM specimens for the cross-sectional view were prepared by mechanical polishing and argon ion beam milling. Raman spectroscopy and X-ray photoelectron spectroscopy (XPS) tests were conducted to further analyze the nanostructural changing caused by oxygen plasma etching. Raman spectra between 1100 cm^{-1} and 3500 cm^{-1} were recorded by HORIBA HR800 laser confocal Raman spectrometer with the excitation laser length of 514 nm. An AXIS ultra DLD multifunctional XPS with a monochromatic Al Kα X-ray source was used to analyze the chemical compositions and bonding configurations.

The surface morphologies were characterized by an Innova atomic force microscopy (AFM) system with scan size of 5 μm × 5 μm, and the measurements were repeated three times on each sample. The nanoindentation tests were performed using a Hysitron TI 900 Triboindenter equipped with a 200-nm-radius Berkovich diamond tip on the carbon films. A quartz standard sample was used for calibration. The maximum load was 1 mN. The hardness was calculated by Oliver-Pharr method. Three measurements on different positions of the film were repeated to ensure the experimental accuracy. A Bruker Dimension Edge scanning probe microscope (SPM) system was employed to compare the scratch behavior of the carbon films. Each sample surface was laterally scratched at three different locations with a 40-nm-radius diamond tip at a normal load of 40 μN, and then the scratched surfaces were scanned with the same tip. Then at eight different positions of these three scratch tracks, the cross-sectional topographies across the scratches were measured to calculate the mean value and standard deviation of the scratch depth. The scratch resistance was evaluated by comparing the scratch depths of different carbon films. A Pin-on-Disk Tribometer was used to study the tribological properties of the carbon films. The tribotests of the carbon films sliding against a Si_3N_4 ball (radius of 3.17 mm) were performed with normal load of 2 N, disk rotational speed of 180 rpm and frictional radius of 1.4 mm. Five measurements were repeated on each sample. All tribological tests were operated at room temperature (24–25 °C) and a relative humidity of 40–60%.

In order to study whether the oxygen plasma etching could affect the electrical and magnetic properties of the GSEC film, the electrical resistivity of the carbon films was measured by four-point-probe method, and the magnetization measurements were carried out with a Quantum Designs MPMS-XL7 superconductivity

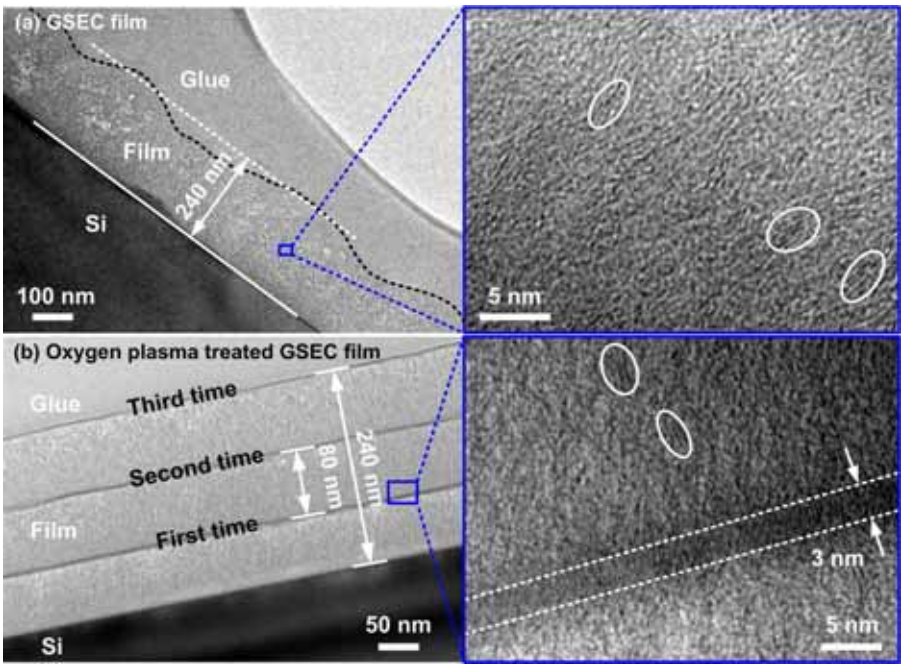

Fig. 2. Cross-sectional TEM images of (a) GSEC film and (b) oxygen plasma treated GSEC film. (For interpretation of the references to color in the text, the reader is referred to the web version of this article.)

quantum interference device (SQUID) magnetometer at 300 K with an applied magnetic field of between −10 kOe and 10 kOe.

3. Results

3.1. Nanostructure

Fig. 2 presents the cross-sectional TEM images of the GSEC film and the oxygen plasma treated GSEC film. In Fig. 2(a), the film thickness was around 240 nm and the film surface was rough containing a lot of asperities. In the enlarged view (blue frame in Fig. 2(a)), it can be seen that graphene sheets distributed uniformly in the amorphous carbon matrix and vertically oriented to the substrate surface. In Fig. 2(b), the thickness of the oxygen plasma treated GSEC film was 240 nm, comparable to that of the GSEC film. And the film surface was smoother without apparent asperities. This film was divided into three parts, and every part contained one bright zone and one dark zone with total thickness of about 80 nm. The three parts corresponded to the three-time oxygen plasma etching processes. Owing to the fact that the plasma etching could only affect the uppermost layer [22], the lower bright zone exhibited the same nanostructure with the GSEC film, containing vertically oriented graphene sheets, and was named as the graphene sheets embedded zone. While the upper dark zone with thickness of around 3 nm was restructured by the oxygen plasma etching and named as the restructured zone. The change of image contrast in the restructured zones suggested that these zones possessed the higher density than the graphene sheets embedded zones [23]. These phenomena indicate that the oxygen plasma etching does not change the nanostructure of the graphene sheets embedded zones and just restructure the 3 nm thick zones.

In order to further explore the nanostructural changing in the restructured zones, Raman spectroscopy tests were performed to analyze the graphene nanocrystallite size in the carbon films. Fig. 3 shows the Raman spectra of the GSEC film and the oxygen plasma treated GSEC film. The peaks at around 1350 cm^{-1}, 1580 cm^{-1}, 2700 cm^{-1} represent D band, G band, 2D band, respectively. And the D band and G band were fitted with a Lorentzian peak and a

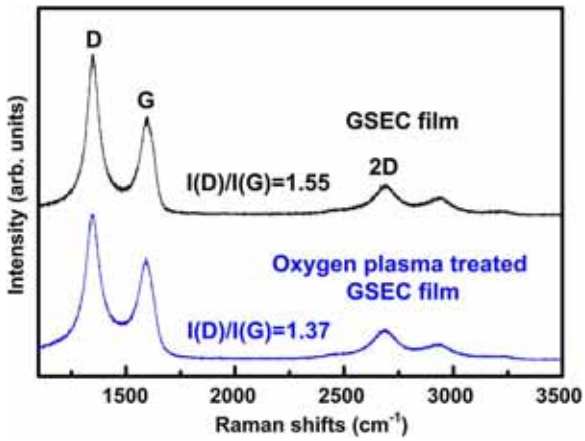

Fig. 3. Raman spectra of GSEC film and oxygen plasma treated GSEC film.

Breit-Fano-Wagner (BFW) peak, respectively [24]. Compared with the GSEC film, the D band and G band of the oxygen plasma treated GSEC film were a little broader and the intensity ratio of D band and G band I_D/I_G decreased from 1.55 to 1.37, indicating the graphene nanocrystallite size in the restructured zones decreases slightly. It should be pointed out that the changes in band widths and I_D/I_G caused by plasma treatment were not large, which was because Raman spectroscopy tests with the large laser penetration depth reflected the average size of graphene nanocrystallites in whole carbon films and the restructured zones were only around 4% of the whole oxygen plasma treated GSEC film. Hence the intrinsic change of the graphene nanocrystallite size in the restructured zones caused by oxygen plasma etching is expected to be much larger.

Owing to the shallower measurement depth of a few nanometers, XPS tests were performed to specify the changes of chemical composition and bonding configuration in the restructured zones. The XPS survey spectra of carbon films showed that the O/C atomic ratios of the GSEC film and the oxygen plasma treated GSEC film

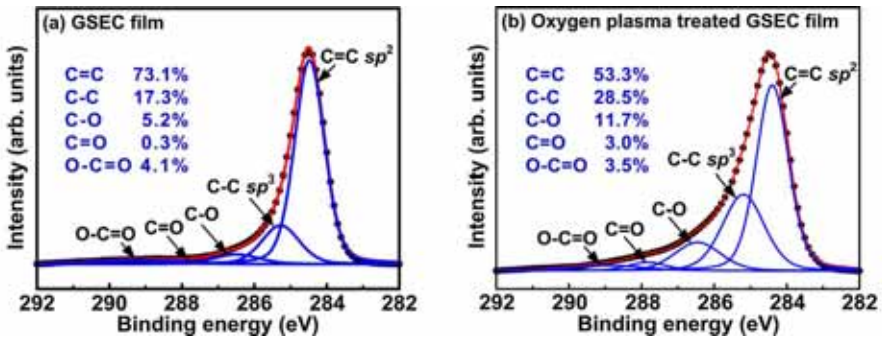

Fig. 4. C 1s XPS spectra of (a) GSEC film and (b) oxygen plasma treated GSEC film. (black dots: original data; red lines: the peak fitting curves; blue lines: five components). (For interpretation of the references to color in this figure legend, the reader is referred to the web version of this article.)

were 0.02 and 0.10, respectively. It indicates that in the restructured zones, there could be more oxygen atoms adsorbed and bonded with the carbon atoms. To examine the bonding configuration change caused by oxygen atom incorporation, the C 1s XPS spectra were fitted by five Gaussian–Lorentzian components after the inelastic scattering backgrounds were subtracted using Shirley's method. The two main components around 284.5 and 285.3 eV correspond to sp^2 and sp^3 carbon hybridization. The remaining three components around 286.5, 287.8 and 288.9 eV are attributed to C—O, C═O and O—C═O [25–27]. The results are shown in Fig. 4. According to the peak integrated area ratios of different bonds, the contents of the five bond types in carbon films are also presented in Fig. 4. The data showed that after oxygen plasma etching, the C═C (sp^2) content decreased from 73.1% to 53.3%, while the C—C (sp^3) content increased from 17.3% to 28.5%. And the C—O content also increased from 5.2% to 11.7% obviously. These results demonstrate that the oxygen plasma treatment induce the increase of the sp^3 bond in the restructured zones.

3.2. Surface roughness

Fig. 5 shows the typical surface topographies of the carbon films. In the GSEC film, the film surface was covered with numerous asperities and the average surface roughness was 20.8 ± 1.1 nm. Such large surface roughness could be attributed to the fact that during the film deposition, the electron irradiation induced the growth of graphene sheets, which has been reported to result in surface roughing [8,9]. On the other hand, the electron bombardment was insufficient to smooth the surface through displacing carbon atoms, leading to considerable rough surface. After the three-time oxygen plasma etching, the average surface roughness of the carbon film decreased to 1.9 ± 0.1 nm, less than one tenth of the former. The reason was that the oxygen plasma with ion kinetic energy of 100 eV could not only sputter carbon atoms within surface asperities physically, but also react with asperity atoms chemically. Therefore, it can be concluded that the oxygen plasma treatment can etch protruding regions of the GSEC film and significantly smooth the surface, which is also confirmed by TEM observation.

3.3. Mechanical properties

After the oxygen plasma etching, the restructured zones had higher sp^3 bond fraction, which may show better mechanical properties. To evaluate the change of mechanical properties caused by oxygen plasma treatment, nanoindentation and nanoscratch tests were conducted on the carbon films. Fig. 6 presents the typical nanoindentation load–displacement curves of the carbon films. After calculation, the hardness of the GSEC film and the oxygen plasma treated GSEC film were 2.3 ± 0.1 GPa and 2.9 ± 0.1 GPa, respectively. Since the maximum penetration depth was beyond one tenth of the film thickness, the value of hardness was considered as a combination of film and substrate. The result proves that after oxygen plasma treatment, the hardness of the restructured zones increases. Because the nanoindentation tests compared the mechanical properties of the whole carbon films, and the restructured zones were only around 4% of the whole oxygen plasma treated GSEC film, the hardness in the restructured zones caused by oxygen plasma etching was expected to be much higher.

Fig. 7 presents an example of the cross-sectional topographies across the scratches (as shown in inset of Fig. 7) of two carbon films after the nanoscratch tests. As a consequence, the scratch depth of the GSEC film was 64.5 ± 5.4 nm, and the scratch depth of the oxygen plasma treated GSEC film decreased to 9.9 ± 0.9 nm. It indicates that the scratch resistance in the restructured zones is improved significantly.

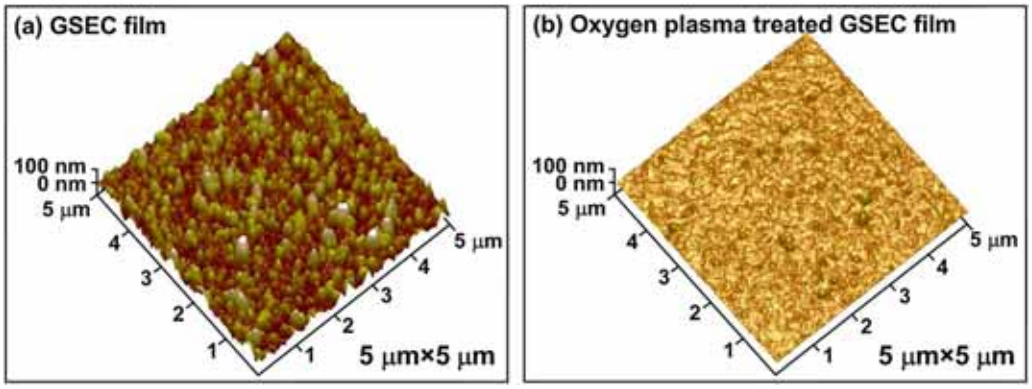

Fig. 5. Typical surface topographies of (a) GSEC film and (b) oxygen plasma treated GSEC film.

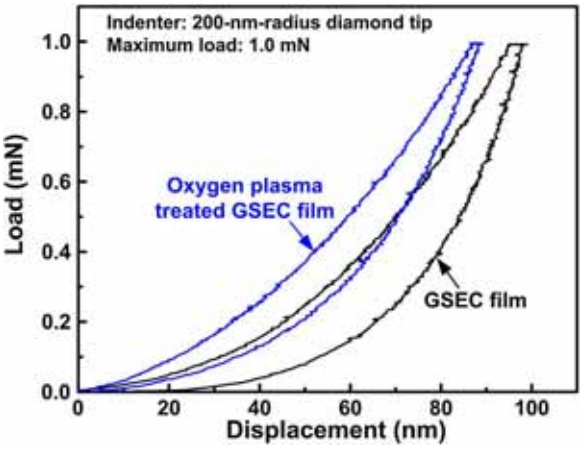

Fig. 6. Typical load–displacement curves of GSEC film and oxygen plasma treated GSEC film.

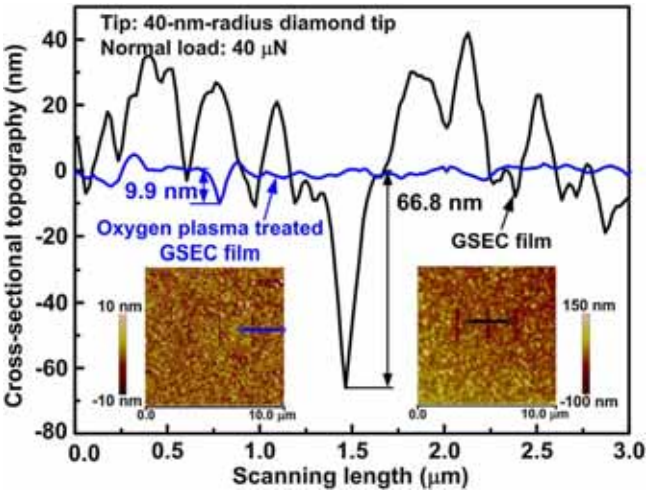

Fig. 7. An example of cross-sectional topographies across the scratches of GSEC film and oxygen plasma treated GSEC film.

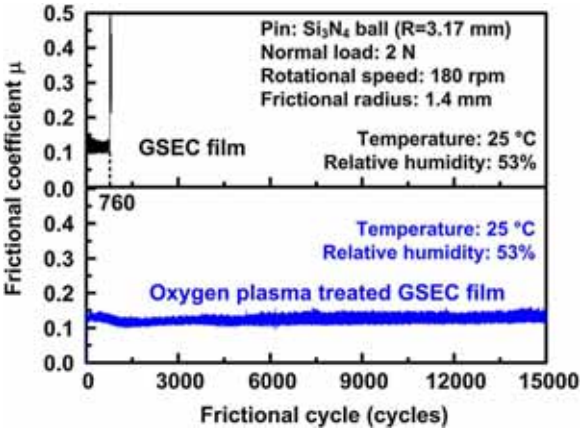

Fig. 8. Typical fiction curves of GSEC film and oxygen plasma treated GSEC film.

3.4. Tribological properties

Fig. 8 shows one group of friction curves of the carbon films among five measurements. For the GSEC film, the mean value of the frictional coefficient was 0.11 and showed a sudden rise after 760 cycles, which means the failure of the film. Such wear resistance is unable to meet the use requirement in nano devices. For the oxygen plasma treated GSEC film, the mean value of the frictional coefficient was kept at about 0.11 and the film cannot be worn out at 15,000 cycles. After five tribological tests, the mean frictional coefficient, wear life together with temperature and relative humidity during each test are also presented in Table 1. The results showed that the mean frictional coefficient of the GSEC film was 0.12 ± 0.01, and its wear life was 930 ± 390 cycles. After the oxygen plasma treatment, the mean frictional coefficient of the oxygen plasma treated GSEC film was 0.11 ± 0.01, and the wear life of five measurements were all more than 15,000 cycles. That is, after the oxygen plasma treatment, the frictional coefficient of the carbon film had no remarkable change, but the wear life dramatically increased from 930 ± 390 cycles to more than 15,000 cycles. Therefore, it turns out that the oxygen plasma treatment can improve the tribological properties of the GSEC film greatly.

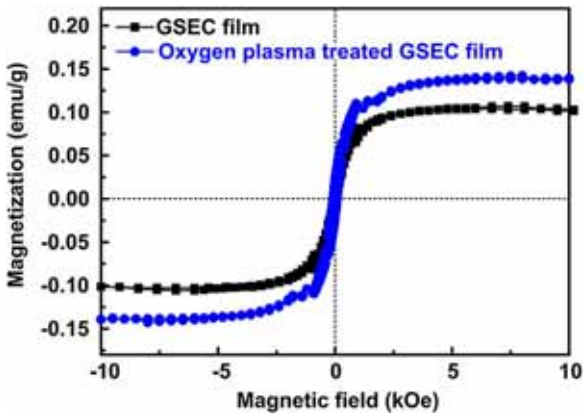

Fig. 9. Magnetic hysteresis loops of GSEC film and oxygen plasma treated GSEC film.

The increase in the wear life of the carbon film after the oxygen plasma treatment was suggested to be mainly related to two factors. First, the surface roughness of the oxygen plasma treated GSEC film was less than one tenth of that of the GSEC film. In general, if the carbon film is rougher, a higher level of mechanical interlocking would take place between surface asperities and lead to higher frictional losses [28]. Thus the smoother surface made the oxygen plasma treated GSEC film get a longer wear life. Second, after the oxygen plasma etching, the hardness and scratch resistance in the restructured zones were improved significantly. The enhancement in mechanical properties could play an important role in the ability of the carbon film to carry load and hence resist wear, extending the wear life of the film. Thus the combined effect of the lower surface roughness and the enhanced mechanical properties made the oxygen plasma treated GSEC film possess a much longer wear life in comparison with the GSEC film.

4. Discussions

The GSEC film has been proved to have high electrical conductivity and strong magnetism [11,12]. In order to further explore whether the oxygen plasma treatment weakened these properties, the electrical resistivity and saturation magnetization of the carbon films were compared. The electrical resistivity of the GSEC film was 0.015 Ω cm. After the oxygen plasma treatment, the electrical resistivity of the film was 0.017 Ω cm, almost no change. It was because after the plasma etching, the graphene sheets embedded zones were still in the majority, which play a significant role in conducting electricity. The magnetic hysteresis loops of the carbon films are presented in Fig. 9. For the GSEC film, the saturation magnetization was 0.10 emu/g. After the oxygen plasma treatment, the saturation magnetization of the film increased to 0.14 emu/g.

Table 1
Mean frictional coefficient, wear life together with temperature and relative humidity of five tribological tests on GSEC film, and oxygen plasma treated GSEC film.

Sample	GSEC film				
	1	2	3	4	5
Mean frictional coefficient	0.11	0.11	0.14	0.12	0.13
Wear life (Cycles)	760	830	490	1520	1070
Temperature (°C)	25	25	25	24	25
Relative humidity (%)	53	50	54	53	48
Sample	Oxygen plasma treated GSEC film				
	1	2	3	4	5
Mean frictional coefficient	0.11	0.12	0.12	0.11	0.11
Wear life (Cycles)	>15,000	>15,000	>15,000	>15,000	>15,000
Temperature (°C)	25	25	25	25	25
Relative humidity (%)	53	50	53	53	49

The strong magnetism of the GSEC film was ascribed to the spin magnetic moment at the graphene sheet edges in nanocrystallites, and small size but dense nanocrystallites were beneficial for strong magnetization since they provided a large amount of graphene sheet edges [29]. The slight increase in saturation magnetization was inferred to result from the more graphene sheet edges in the restructured zones induced by the smaller graphene nanocrystallite size. Therefore, the oxygen plasma treatment retains the outstanding electrical and magnetic properties of the GSEC film.

5. Conclusions

For improving the tribological properties of the graphene sheets embedded carbon (GSEC) film, the 3 nm thick graphene nanocrystallite films were implanted in the film by the oxygen plasma etching technique during the film deposition. The oxygen plasma etched film showed much smoother surface, higher hardness, higher nanoscratch resistance and longer wear life than the unetched GSEC film. The origin of these improved properties was ascribed to the 3 nm thick restructured film. In addition, the oxygen plasma treated GSEC film retained the high electrical conductivity and strong magnetism. These findings can be expected for fabricating a nanostructured carbon film in possession of excellent electrical, magnetic and tribological properties for potential applications in novel carbon based nano devices.

Acknowledgments

The authors would like to thank the National Natural Science Foundation Major Research Program on Nanomanufacturing under Grant Number of 91323303, the National Natural Science Foundation of China under Grant Number of 51575359, and Research Fund for the Doctoral Program of Higher Education of China under Grant Number of 20120201110029.

References

[1] F. Schwierz, Graphene transistors, Nat. Nanotechnol. 5 (2010) 487–496.
[2] M. Scarselli, P. Castrucci, M. De Crescenzi, Electronic and optoelectronic nano-devices based on carbon nanotubes, J. Phys. Condens. Matter 24 (2012) 313202.
[3] D.S. Grierson, R.W. Carpick, Nanotribology of carbon-based materials, Nanotoday 2 (2007) 12–21.
[4] C.A. Charitidis, Nanomechanical and nanotribological properties of carbon-based thin films: a review, Int. J. Refract. Met. Hard Mater. 28 (2010) 51–70.
[5] M. Shakerzadeh, G.C. Loh, N. Xu, W.L. Chow, C.W. Tan, C. Lu, R.C.C. Yap, D. Tan, S.H. Tsang, E.H.T. Teo, B.K. Tay, Re-ordering chaotic carbon: origins and application of textured carbon, Adv. Mater. 24 (2012) 4112–4123.
[6] F.J. Flores-Ruiz, C.I. Enriquez-Flores, F. Chiñas-Castillo, F.J. Espinoza-Beltrán, Nanotribological performance of fullerene-like carbon nitride films, Appl. Surf. Sci. 314 (2014) 193–198.
[7] H. Zanin, P.W. May, M.H.M.O. Hamanaka, E.J. Corat, Field emission from hybrid diamond-like carbon and carbon nanotube composite structures, ACS Appl. Mater. Interfaces 5 (2013) 12238–12243.
[8] X.L. Peng, Z.H. Barber, T.W. Clyne, Surface roughness of diamond-like carbon films prepared using various techniques, Surf. Coat. Technol. 138 (2001) 23–32.
[9] O.V. Penkov, V.E. Pukha, E.N. Zubarev, S.S. Yoo, D.E. Kim, Tribological properties of nanostructured DLC coatings deposited by C_{60} ion beam, Tribol. Int. 60 (2013) 127–135.
[10] A. Erdemir, C. Donnet, Tribology of diamond-like carbon films: recent progress and future prospects, J. Phys. D: Appl. Phys. 39 (2006) R311.
[11] C. Wang, D.F. Diao, X. Fan, C. Chen, Graphene sheets embedded carbon film prepared by electron irradiation in electron cyclotron resonance plasma, Appl. Phys. Lett. 100 (2012) 231909.
[12] C. Wang, D.F. Diao, Magnetic behavior of graphene sheets embedded carbon film originated from graphene nanocrystallite, Appl. Phys. Lett. 102 (2013) 052402.
[13] C. Wang, D.F. Diao, Cross-linked graphene layer embedded carbon film prepared using electron irradiation in ECR plasma sputtering, Surf. Coat. Technol. 206 (2011) 1899–1904.
[14] T. Gokus, R.R. Nair, A. Bonetti, M. Bohmler, A. Lombardo, K.S. Novoselov, A.K. Geim, A.C. Ferrari, A. Hartschuh, Making graphene luminescent by oxygen plasma treatment, ACS Nano 3 (2009) 3963–3968.
[15] D.Y. Yun, W.S. Choi, Y.S. Park, B. Hong, Effect of H_2 and O_2 plasma etching treatment on the surface of diamond-like carbon thin film, Appl. Surf. Sci. 254 (2008) 7925–7928.
[16] F.R. Marciano, L.F. Bonetti, N.S. Da-Silva, E.J. Corat, V.J. Trava-Airoldi, Wettability and antibacterial activity of modified diamond-like carbon films, Appl. Surf. Sci. 255 (2009) 8377–8382.
[17] D.C. Kim, D.Y. Jeon, H.J. Chung, Y. Woo, J.K. Shin, S. Seo, The structural and electrical evolution of graphene by oxygen plasma-induced disorder, Nanotechnology 20 (2009) 375703.
[18] L. Jiang, A.G. Fitzgerald, M.J. Rose, R. Cheung, B. Rong, E. Van der Drift, X-ray photoelectron spectroscopy studies of the effects of plasma etching on amorphous carbon nitride films, Appl. Surf. Sci. 193 (2002) 144–148.
[19] X. Zheng, Z. Ma, L. Zhang, J. Wang, Investigation on the etching of thick diamond film and etching as a pretreatment for mechanical polishing, Diamond Relat. Mater. 16 (2007) 1500–1509.
[20] M.L. Guo, D.F. Diao, X. Fan, L. Yang, L.W. Yu, Scratch behavior of re-structured carbon coating by oxygen plasma etching technology for magnetic disk application, Surf. Coat. Technol. 251 (2014) 128–134.
[21] X. Fan, D.F. Diao, K. Wang, C. Wang, Multi-functional ECR plasma sputtering system for preparing amorphous carbon and Al–O–Si films, Surf. Coat. Technol. 206 (2011) 1963–1970.
[22] P. Solis-Fernandez, J.I. Paredes, A. Cosío, A. Martínez-Alonso, J.M.D. Tascón, A comparison between physically and chemically driven etching in the oxidation of graphite surfaces, J. Colloid Interf. Sci. 344 (2010) 451–459.
[23] D.G. McCulloch, J.L. Peng, D.R. McKenzie, S.P. Lau, D. Sheeja, B.K. Tay, Mechanisms for the behavior of carbon films during annealing, Phys. Rev. B 70 (2004) 085406.
[24] A.C. Ferrari, J. Robertson, Interpretation of Raman spectra of disordered and amorphous carbon, Phys. Rev. B 61 (2000) 14095.
[25] S. Stankovich, D.A. Dikin, R.D. Piner, K.A. Kohlhaas, A. Kleinhammes, Y. Jia, Y. Wu, S.T. Nguyen, R.S. Ruoff, Synthesis of graphene-based nanosheets via chemical reduction of exfoliated graphite oxide, Carbon 45 (2007) 1558–1565.
[26] D.R. Dreyer, S. Park, C.W. Bielawski, R.S. Ruoff, The chemistry of graphene oxide, Chem. Soc. Rev. 39 (2010) 228–240.
[27] S. Park, K.S. Lee, G. Bozoklu, W. Cai, S.T. Nguyen, R.S. Ruoff, Graphene oxide papers modified by divalent ions-enhancing mechanical properties via chemical cross-linking, ACS Nano 2 (2008) 572–578.
[28] C. Chen, D.F. Diao, X. Fan, L. Yang, C. Wang, Frictional behavior of carbon film embedded with controlling-sized graphene nanocrystallites, Tribol. Lett. 55 (2014) 429–435.
[29] C. Wang, X. Zhang, D.F. Diao, Nanosized graphene crystallite induced strong magnetism in pure carbon films, Nanoscale 7 (2015) 4475–4481.